Effect of high-pressure oxygen annealing in promoting superconductivity in $YSr_2Cu_{2.7}Fe_{0.3}O_y$: Evidence for Fe coordination number change in the chains

F. Shi, W. J. Bresser, and M. Zhang
Department of Electrical and Computer Engineering and Computer Science, University of Cincinnati, Cincinnati, Ohio 45221-0030

Y. Wu
Department of Electrical and Computer Engineering and Computer Science, University of Cincinnati, Cincinnati, Ohio 45221-0030 and Sony, Inc., San Antonio, Texas 78245

D. McDaniel
Department of Chemistry, University of Cincinnati, Cincinnati, Ohio 45221-0172

P. Boolchand
Department of Electrical and Computer Engineering and Computer Science, University of Cincinnati, Cincinnati, Ohio 45221-0030
(Received 20 February 1996)

A superconducting transition temperature (T_c) of 60 K and a shielding fraction (V_{sh}) of nearly 100% is achieved in tetragonal $YSr_2Cu_{2.7}Fe_{0.3}O_y$ samples only after high pressure (27 MPa) oxygen annealing at 915 °C. On the other hand, samples synthesized at ambient pressure become barely superconducting ($T_c^{max} \simeq 30$ K, $V_{sh} \simeq 4\%$) even after prolonged annealing in an oxygen ambient. ^{57}Fe Mössbauer spectroscopy measurements suggest that in samples synthesized at ambient pressure, Fe cations localized in the chains are present in metastable corner-sharing tetrahedral units (site A). At high oxygen pressures these sites (A) trap oxygen locally to form distorted trigonal bipyramid units (site C) which promote superconductivity as revealed by magnetization measurements. Fe cations at site C act as effective flux-pinning sites, with such samples displaying not only a large intragrain critical current (J_c^m) but also a secondary peak in J_c^m at a finite external field characteristic of flux pinning in a quasi-two-dimensional material. [S0163-1829(96)06833-6]

I. INTRODUCTION

Unlike $YBa_2Cu_3O_7$ (YBCO), its Sr analog $YSr_2Cu_3O_7$ (YSCO) with a $T_c = 60$ K can only be synthesized at rather high oxygen pressure.[1] Recently, a flurry of activity in this layered cuprate was stimulated by the general recognition[2–7] that a variety of metal dopants (M) can replace Cu(1) chain sites in the $P4/mmm$ host structure to stabilize the superconducting phase in $YSr_2(Cu_{1-x}M_x)_3O_y$ samples at ambient pressure. Several groups[2–7] have reported superconductivity with M=Fe, and $x = 0.10$, at $T_c \simeq 30$ K. Such samples interested us because in addition to probing structural, magnetic, and superconducting properties using conventional methods, one could also track the metal dopant (Fe) local chemistry as a function of sample processing using Mössbauer spectroscopy.

Pure YBCO samples with a $T_c = 90$ K and a shielding fraction of nearly 100% are now routinely synthesized under standard conditions of annealing, i.e., one atmosphere of oxygen or air. On the other hand, in metal-doped YBCO samples with M=trivalent species such as Al^{3+}, Fe^{3+}, Co^{3+} synthesized under standard annealing condition, superconductivity disappears ($T_c \rightarrow 0$) progressively as the metal dopant concentrations approaches[8] $x \rightarrow 0.15$. The underlying variation of $T_c(x)$ appears to be an artifact of processing, and does not represent the intrinsic behavior of the system as will become clear from the present work. For example, annealing such samples in an oxygen ambient at high pressures and temperatures restores superconducting properties such as T_c, Meissner fraction (V_m), and critical currents (J_c) in a remarkable fashion. In this work, we will show that the microscopic origin of this behavior can be traced to an Fe coordination number change from 4 (quasitetrahedral) to 5 (trigonal bipyramidal) in the chains. Specifically, Fe-doped YSCO samples at $x = 0.10$ synthesized under standard annealing conditions possess a $T_c = 30$ K, a shielding fraction of 4% and a trimodal (A, B, and C) distribution of Fe cation sites. Two of these sites (A,C) represent Fe localized in the chains while the third one (B) represents Fe present in the planes. Such samples when annealed at 915 °C in high oxygen pressure (27 MPa) are not only stable when brought back to laboratory ambient, but display a $T_c = 60$ K, a shielding fraction of ~100% and an almost unimodal distribution of Fe sites (site C) in the chains. The atomic-scale structural changes taking place in the chains upon oxygen uptake strongly suggest that Fe bearing trigonal bipyramidal chain sites (site C) represent a necessary structural element to support superconductivity in the present metal-doped trilayered cuprate system.

II. EXPERIMENTAL PROCEDURE AND RESULTS

A. Sample preparation

$YSr_2Cu_{2.7}Fe_{0.3}O_y$ (YSCFO) samples were prepared by standard solid-state reaction in two steps. In step one, fine

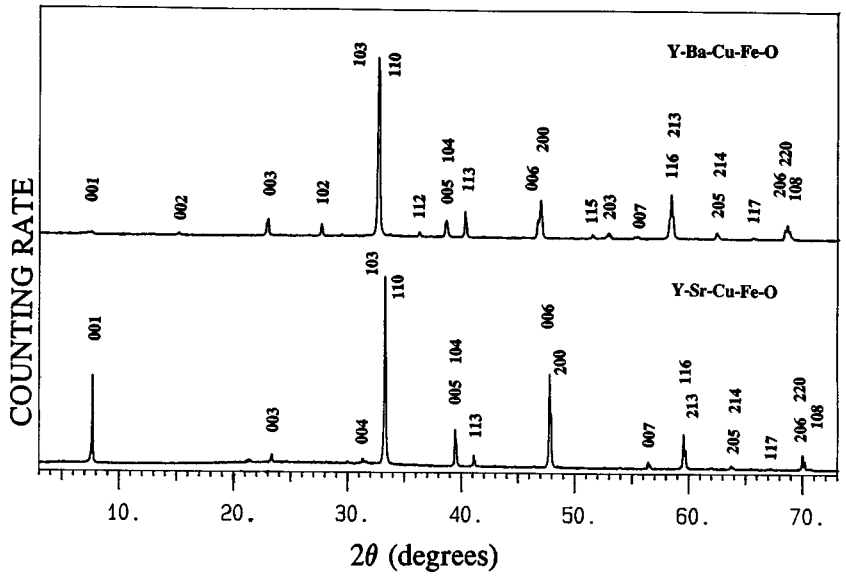

FIG. 1. Powder XRD scans of $YSr_2Cu_{2.7}Fe_{0.3}O_{7.3}$ sample (HPO3) compared to its Ba analog.

grained ($<5\ \mu$) high-purity powders of Y_2O_3, $SrCO_3$, CuO, Fe_2O_3, and enriched $^{57}Fe_2O_3$ were thoroughly mixed in the desired ratio and heated in air at a temperature T in the range $900\,°C<T<1050\,°C$, for at least 48 h with a few intermediate grindings and/or pelletizing resulting in the precursor. In step two, the precursor was reacted in a high-pressure oxygen ambient (27 MPa) at 915 °C for 24 h, employing an autoclave assembly described earlier.[9] Typically, about 300 mg of the precursor was wrapped in gold foil and flushed with high-purity O_2 in the autoclave. The sample was next heated at a rate of 20 °C/min to 915 °C, held at that temperature for 24 h and then cooled to 100 °C at a rate of 1 °C/min. In some cases the precursor was heated in flowing oxygen at 1 atm for periods t in the range $24\ h<t<78$ h to afford a comparison of physical properties of the resulting sample with those of the high O_2 pressure-processed samples. Seven samples following the above protocol will be reported upon in this paper. Specific details on sample processing will be outlined in the paper appropriately when discussing results on these samples.

B. Powder x-ray-diffraction (XRD)

Phase purity and structure of the samples were analyzed by means of a Rigaku (model D/Max 2100 H) x-ray powder diffractometer using Cu $K\alpha$ radiation. Diffraction scans were performed at room temperature over the angular range $3°\leqslant 2\theta\leqslant 73°$ with a step size of 0.02° and a counting time of 6 s per step. In some cases a step of 0.002° and a counting time of 30 s per step was also used to collect data in the range $46°\leqslant 2\theta\leqslant 49°$. Lattice parameters were determined by fitting the peak positions of at least 15 reflections using a standard least-squares reduction method.

The precursor formed after step 1 upon sintering in air (sample A) is found to be a single phase (orthorhombic-space group $Pmmm$) material as revealed by powder x-ray diffraction (XRD). Further heat treatment of the precursor in an oxygen ambient of 1 atm (sample O) or at high pressures (sample HPO3) does not lead to appearance of any observable impurity phase. Figure 1 shows a typical XRD pattern of sample HPO3. The pattern was indexed on space group $P4/mmm$ with a tetragonal cell (TII). A precursor sample quenched from 1020 °C into liquid nitrogen (sample Q) was also prepared and found to be tetragonal (TI). XRD scans of the various samples (Q, A, O, HPO3) in the $46°\leqslant 2\theta\leqslant 49°$ range (Fig. 2) reveal the (020), (006), and (200) reflects move systematically to higher angles and also provide direct evidence of structural phase transitions upon progressive oxygenation in the sequence ($Q\rightarrow A\rightarrow O\rightarrow$HPO3). Specifically for sample Q, a tetragonal cell with $a=b=3.816$ Å and $c=11.45$ Å; for sample A an orthorhombic cell with $a=3.813$ Å, $b=3.823$ Å, $c=11.441$ Å; and for sample O a tetragonal cell with $a=b=3.804$ Å, $c=11.417$ Å, were found. For the fully oxygenated sample HPO3, the tetragonal cell parameters were found to be $a=3.798$ Å, $c=11.395$ Å. The lattice parameters are plotted as a function of oxygen content in Figs. 3(a) and 3(b) and show that the c-cell length decreases almost linearly with oxygen content. Furthermore, in the present YSCFO system, a $T(\mathrm{I})\rightarrow O\rightarrow T(\mathrm{II})$ structural transition is also observed as the oxygen content increases.

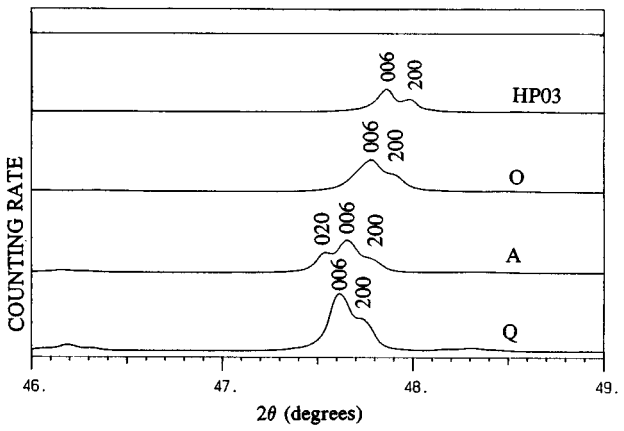

FIG. 2. Tetragonal I→Orthorhombic→Tetragonal II phase transformations in $YSr_2Cu_{2.7}Fe_{0.3}O_y$ as a function of increasing oxygen content in the sequence $Q\rightarrow A\rightarrow O\rightarrow$HPO3.

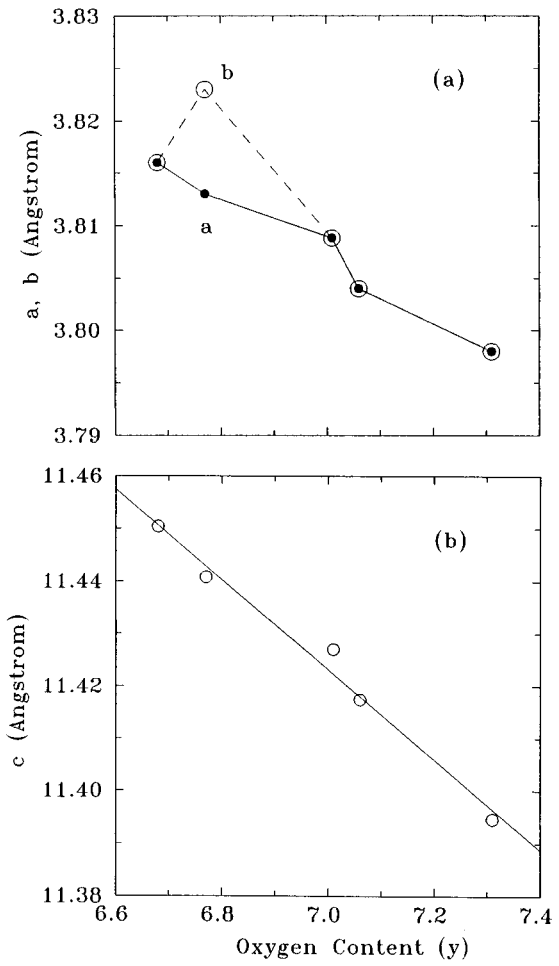

FIG. 3. Lattice parameters of $YSr_2Cu_{2.7}Fe_{0.3}O_y$ samples (a) a,b cell lengths and (b) c cell length plotted as a function of oxygen content y.

C. Dc magnetization

Dc magnetization of the samples was studied as a function of temperature using an EG&G-PAR model 4500 vibrating sample magnetometer coupled to an APD, Inc. He cryocooler using a DMX-19 shroud. Both Meissner fraction [field-cooled (FC)] and shielding or zero-field-cooling fraction (ZFC) were established. The measured magnetic moment (emu) was normalized to the sample mass to yield the mass magnetization, M(emu/g) as a function of temperature. The Meissner fraction V_m was estimated by using the relation $V_m=(4\pi\rho M/H)$, where ρ is the x-ray density of the material in gm/cm^3, and H is the applied magnetic field in Oe, and M is the mass magnetization. Magnetization hysteresis loops were recorded as a function of the applied field in the range $0<H<1$ T at desired temperatures. From these measurements the T dependence of irreversibility field ($H_{\rm irr}$), and magnetic critical current J_c^m were estimated.

Dc magnetization as a function of temperature for sample HPO3 (shown in Fig. 4) reveals a superconducting transition onset at 60 K. The diamagnetic shielding of this sample equals 90% that of a perfect superconductor. The FC results reveal a Meissner fraction of 42% upon cooling in a 15 Oe field. Figure 4 also shows the temperature dependence of zero-field cooled (ZFC) magnetization for samples A, O, and

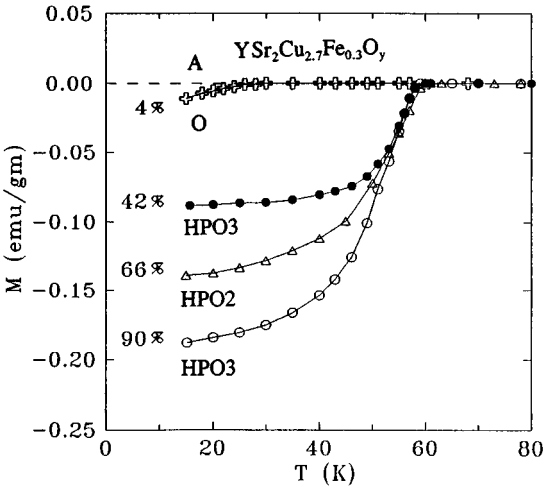

FIG. 4. T dependence of dc magnetization in indicated $YSr_2Cu_{2.7}Fe_{0.3}O_y$ samples. See text for sample labels. The filled circles correspond to a field-cooled (Meissner) sequence, while the open symbols each correspond to a zero-field-cooled (shielding) sequence.

HPO2. The dashed line represents the results for the nonsuperconducting orthorhombic sample A. Sample O, processed in flowing oxygen, displayed a T_c of 30 K and shielding fraction of 4%. T_c's of the samples increased remarkably by high pressure oxygen sintering, up to 60 K, which equals T_c of pristine YSCO. Samples HPO1, HPO2, and HPO3 differed from each other in that the precursor preparation (HPO1: 950–1030 °C/60 h; HPO2: 1000–1040 °C/48 h; HPO3: 1000–1050 °C/48 h) conditions were different. Samples HPO1 and HPO2 have a T_c of 60 K and Meissner fractions of 31.8 and 36.7%, respectively. There is evidence to suggest that porosity of the precursor influences the superconducting volume fraction of the final product.

Figure 5 shows the irreversible magnetization $M(H)$ of sample HPO3 taken at several temperatures. Noteworthy in this figure is the secondary peak at a finite field which moves

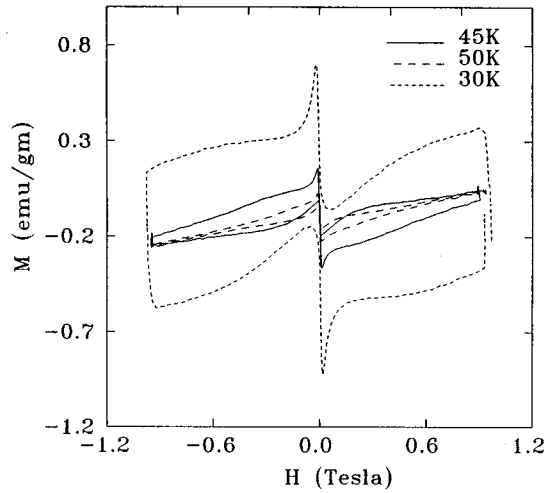

FIG. 5. Magnetization hysteresis loops of HPO3 sample taken at indicated temperatures displaying evidence of a secondary (fishtail) magnetization.

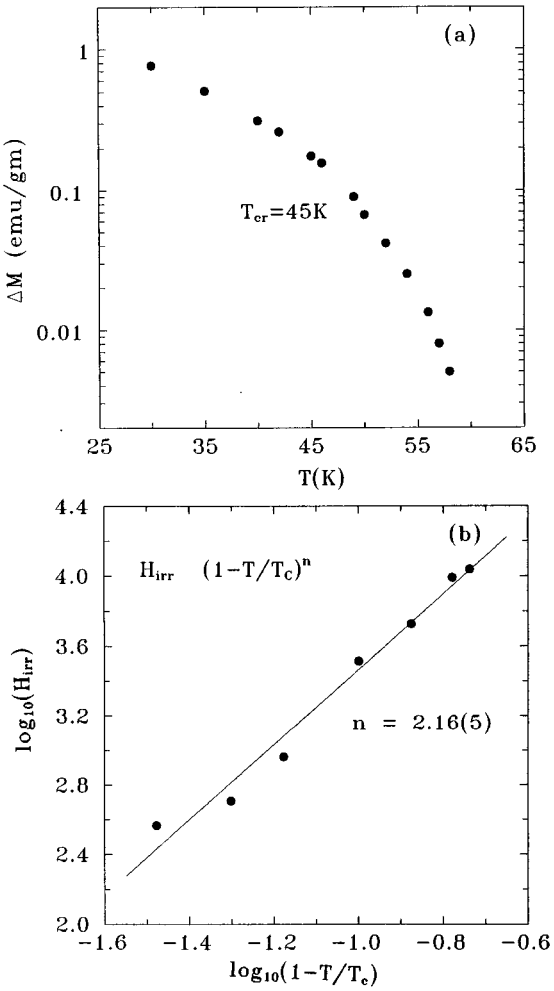

FIG. 6. (a) Log of irreversible magnetization at the secondary peak plotted against T, (b) log of $H_{\rm irr}$ plotted against $\log_{10}(1-T/T_c)$ revealing $n=2.16(10)$. These results pertain to sample HPO3.

to lower fields with increasing temperatures and disappears as T approaches 55 K. This is an observation of the secondary peak in the irreversible magnetization (ΔM) of a sintered polycrystal 123 material. The secondary peak is plotted as a function of temperature in Fig. 6(a). As T is lowered below T_c, ΔM increases sharply at first and then appears to level off and undergo a change in functional form at $T=T_{\rm cr}=45$ K. In the $T_{\rm cr}<T<T_c$ temperature range, the irreversible field $H_{\rm irr}$ is found to vary as $(1-T/T_c)^n$ with $n=2$ power law [see Fig. 6(b)]. We shall return to discuss these results in Sec. III.

D. Thermogravimetric analysis and oxygen content

The thermal stability and the oxygen content of the samples were established by thermogravimetric analysis (TGA) using a Perkin Elmer Model 7 TGA. Typically about 30 mg of a sample was put into a platinum pan and heated from room temperature to 900 °C at a rate of 10 °C/min in a stream of flowing (50 cc/min) argon gas. Oxygen stoichiometry of one of the samples was established directly by gasometric analysis to calibrate the weight loss in a TGA scan

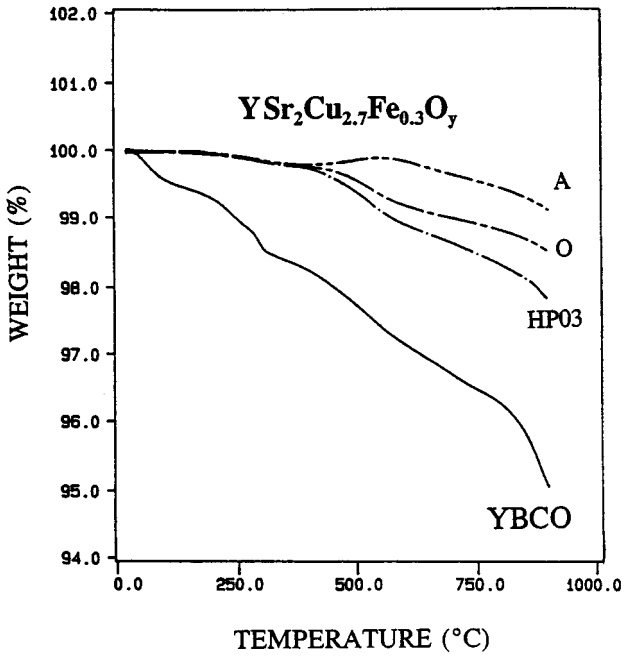

FIG. 7. Thermogravimetric scans of indicated samples taken in an argon gas flow.

and to determine the oxygen content of the samples. In gasometric analysis measurements, a known quantity of the cuprate sample is decomposed by an acid and the volume of oxygen evolved measured. From such measurements one can then establish the oxygen content of the starting material to an accuracy of ± 0.02.

The TGA scans for samples A, O, and HPO3 are compared to a standard YBCO sample in Fig. 7. The weight loss of sample Q, A, O, and HPO3 are 0.41, 0.88, 1.46, and 2.16 %, respectively. These weight losses are much smaller than those of YBCO (4.93%). Moreover, while YBCO sample starts to lose oxygen at $T>100$ °C, YSCFO samples keep nearly a constant weight, i.e., the initial oxygen content, up to 450 °C. The increased stability of the YSCFO samples results from the increased coordination number of the Fe dopant in the chains which brings in additional oxygen. In fact, the superconducting properties of YSCFO samples have been monitored by us for nearly a year, and these display no detectable degradation at laboratory ambient as established by magnetometry. To estimate the oxygen content of the YSCFO samples, we suppose an oxygen stoichiometry of $y=y_o+\Delta y$, where y_o is the stationary oxygen content and Δy the removable part of the oxygen content in the present TGA measurements when samples are heated to 900 °C in Ar. A gasometric analysis of our sample labeled A gave an oxygen content of 6.85(2) and it was used to obtain y_0 as 6.54 ± 0.02. Using this value of y_o the oxygen stoichiometry of samples Q, O, and HPO3, for example, is determined to be 6.68, 7.06, and 7.18, respectively, from the measured TGA weight loss.

E. ^{57}Fe Mössbauer spectroscopy

Spectra of the samples were taken[9] with a standard constant acceleration drive at room temperature using a ^{57}Co in a Rh source and a Kr proportional counter. Spectra were least-squares fit[9] to a superposition of doublets with Lorent-

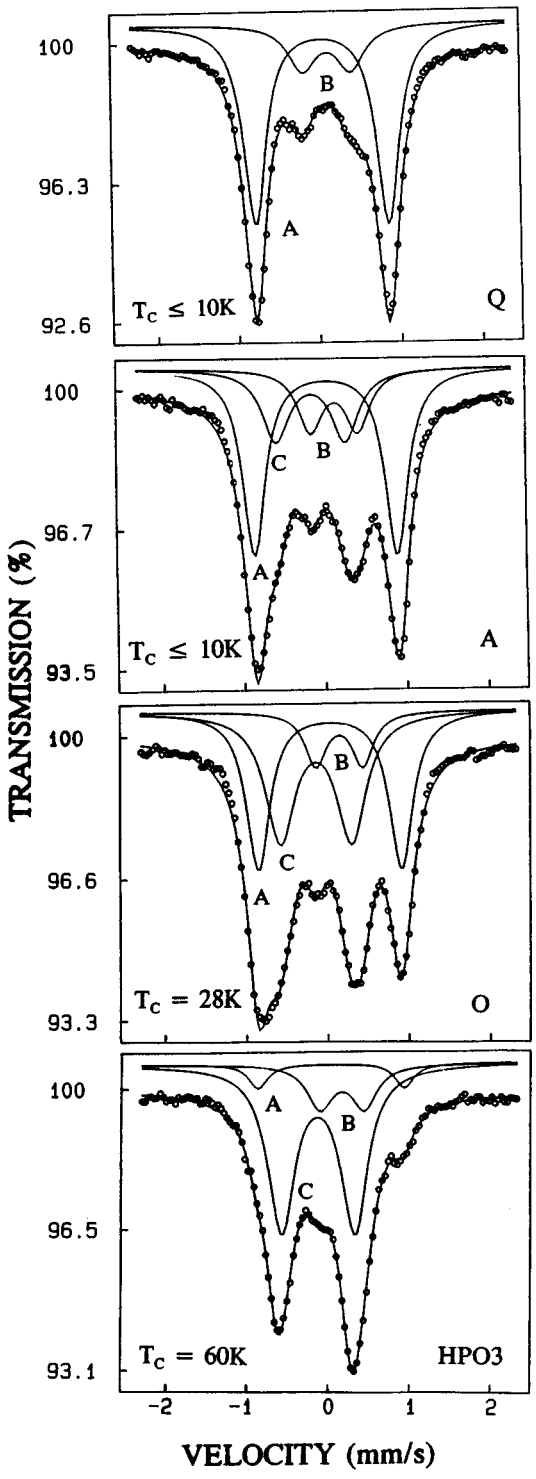

FIG. 8. Room temperature Mössbauer spectra of indicated $YSr_2Cu_{2.7}Fe_{0.3}O_y$ samples showing growth in intensity of *C*-site doublet at the expense of the *A*-site doublet in the sequence $Q \rightarrow A \rightarrow O \rightarrow$HPO3.

zian line shapes possessing variable centroid, splitting, and linewidths. Spectra taken at lower T will be discussed elsewhere.

Figure 8 displays spectra of samples Q, A, O, and HPO3. A line-shape analysis in terms of three doublets (A, B, and C) yielded parameters (δ-isomer shift, Δ-quadrupole splitting) which are summarized in Table I. The site nomenclature is the one used in Ref. 10; A and C represent[5,7,10–14] Fe-chain sites while B represents an Fe-plane site. At the outset, these assignments, suggest that slightly over 80% of the Fe dopant localizes in the chains (Table I) which does not change appreciably with oxygen content. The site parameters are in good agreement with the recent work of Pissas *et al.*[7] and Smith, Taylor, and Thompson[5] on YSCFO samples prepared at ambient oxygen pressure. In the present work, we were able to observe a rather spectacular change in the line shape upon oxygenation of YSCFO samples at high pressures, which can be understood in terms of a systematic growth of C-site intensity at the expense of A-site intensity in the $Q \rightarrow A \rightarrow O \rightarrow$HPO3 sequence (Fig. 8). In particular, the spectrum of the fully oxygenated sample (HPO3) reveals predominantly C-site occupancy with only traces of A-site occupancy. Remarkably, the observed Mössbauer site-intensity ratio $I_C/(I_A+I_C)$ appears to be correlated with sample oxygen content (Fig. 9) and displays two plateaus. In Mössbauer spectroscopy site-integrated intensities I are related to site-occupancies N through the recoil-free-fraction f, i.e., $I=Nf$. The site-intensity ratios become the site occupancies if the site f factors are all the same. We shall return to discuss later the correlation between $I_C/(I_A+I_C)$ and oxygen content in conjunction with the chain molecular structure, and superconductivity.

Mössbauer spectroscopy measurements on grain-aligned YSCFO samples show that Fe does not substitute for Cu(1) chain sites of the host structure. There are plausible reasons to believe that site A in the YSCFO system represents an Fe^{3+} cation present in a distorted-tetrahedral coordination in [110] chains as found for Ga in the model compound $YSr_2Cu_2GaO_7$.[11] Such a site is realized, for example, by starting with a square-planar coordination in the chains [Fig. 10(a)], and having one of the nearest-neighbor O(4) oxygen atoms move to O(5) location accompanied with the displacement of the Fe(1) cation towards the interior of the pseudo-tetrahedron formed by the O(1)×2, O(4)×1, and O(5)×1 oxygen atoms [Fig. 10(b)]. The large quadrupole splitting ($\Delta = 1.79$ mm/s), the negative sign[12,13] of V_{zz}, and the direction of V_{zz} somewhat tilted with respect to the c axis can be reconciled with such an assignment. This assignment[10] is to be preferred over a square-planar one [O(1)×2, O(4)×2] for site A [Fig. 10(a)], since for the latter V_{zz} is expected to be perpendicular to the c axis. Site C is populated in oxygen-rich samples, and it is identified as an Fe^{4+} site that has a distorted trigonal bipyramid coordination in the chains, but not octahedral.[10] Site C local structure probably consists of an additional oxygen trapped near site A in the ab plane. Finally, site B is identified with Fe^{3+} (high-spin, $S=5/2$) present at Cu(2) sites in the planes, probably quasioctahedrally coordinated as discussed elsewhere.[10,14]

III. DISCUSSION

A. Structural transitions in Fe-doped YSCO with oxygen content

Powder x-ray-diffraction scans in high-T_c materials provide an average structure of the samples, with space-group symmetry and lattice parameters. In the present $YSr_2Cu_{2.7}Fe_{0.3}O_y$ samples, we have observed evidence of

TABLE I. Room-temperature Mössbauer effect parameters, δ—isomer shift, Δ—quadrupole splitting, Γ—FWHM, In/I—site intensity ratio in indicated $YSr_2Cu_{2.7}Fe_{0.3}O_y$ samples. See text for details.

Sample	Site	δ [a] (mm/s)	Δ (mm/s)	Γ (mm/s)	I_n/I
Q	*A*:	0.152(1)	1.695(1)	0.34(2)	0.76(2)
	B:	0.219(3)	0.576(6)	0.41(2)	0.23(2)
	C:				
A	*A*:	0.144(2)	1.754(4)	0.31(2)	0.55(2)
	B:	0.251(4)	0.577(8)	0.36(2)	0.25(2)
	C:	−0.030(5)	0.848(9)	0.35(2)	0.20(1)
O	*A*:	0.139(2)	1.766(5)	0.34(2)	0.43(2)
	B:	0.261(5)	0.577(9)	0.41(2)	0.14(2)
	C:	−0.036(5)	0.877(5)	0.39(2)	0.43(2)
HPO3	*A*:	0.142(8)	1.792(17)	0.28(3)	0.08(1)
	B:	0.273(5)	0.544(4)	0.38(2)	0.16(2)
	C:	−0.006(2)	0.899(4)	0.39(1)	0.75(2)

[a]Relative to α-Fe.

two structural transitions as a function of oxygen content y. At $y=6.68$ (sample Q) a tetragonal phase I is observed, which transforms to an orthorhombic phase at an oxygen content $y=6.85$ (sample A). With additional oxygen incorporation into the structure (sample O), at $y=7.06$, a second tetragonal phase II appears.

The tetragonal (I) and orthorhombic phases observed in YSCFO are similar to the tetragonal and orthorhombic (II) phases observed in pristine YBCO. Neutron Bragg scattering results[15] on oxygen-deficient YBCO have shown that in the tetragonal phase I, site occupancies of the oxygen O(4) and O(5) chain sites are found to be nearly equal. With increasing oxygen content ($y>6.5$) stabilization of the orthorhombic phase is ascribed to formation of square-planar chains running along the b axis with near full occupancy of oxygen O(4) sites and the lack of such occupancy for O(5) sites between the chains. However, the tetragonal phase II observed in YSCFO has yet to be established for overdoped pure YBCO. The presence of two types of cations in the

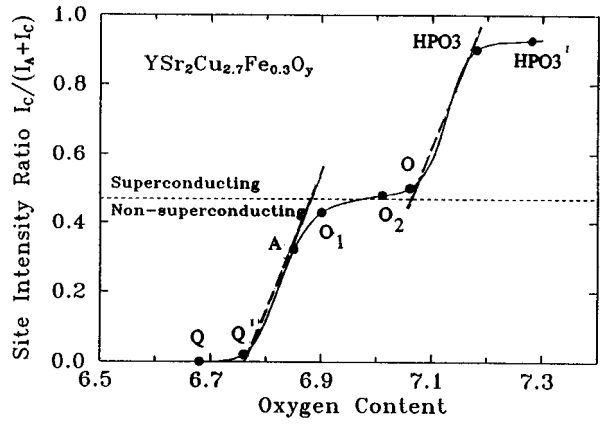

FIG. 9. Mössbauer site intensity ratios $I_C/(I_A+I_C)$ of $YSr_2Cu_{2.7}Fe_{0.3}O_y$ samples plotted as a function of oxygen content y. O_1O_2 and O represent samples annealed in flowing oxygen at 550 °C for 24, 48, and 60 h, respectively. HPO3 and HPO3′ designate samples high-pressure oxygen annealed for 24 and 48 h, respectively. Q and Q' designate precursors quenched from 900 °C in air in a pellet and powdered form, respectively.

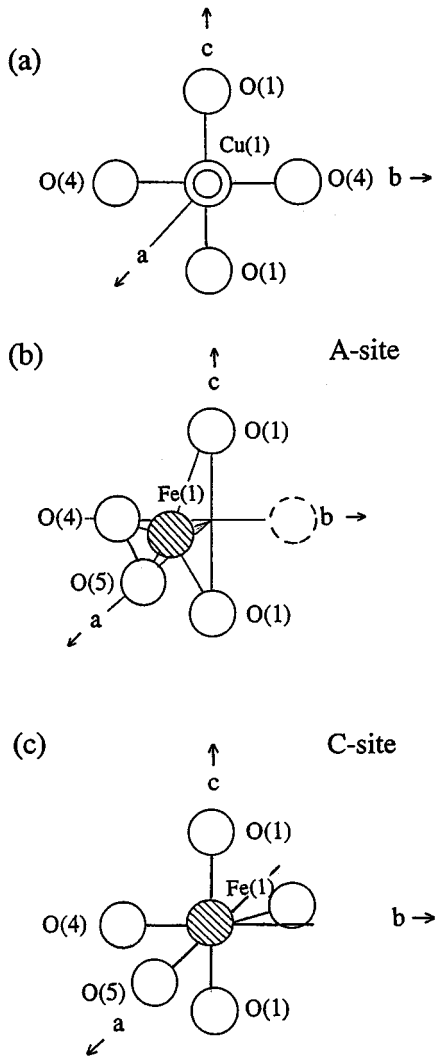

FIG. 10. Local structures of (a) Cu(1) site, (b) Fe(1) A site and (c) Fe(1) C site in YBCO or YSCO. Absorption of oxygen at the O(4) site and relocation of Fe(1) in the center, converts the tetrahedral A site into a trigonal bipyramidal C site.

approximate ratio of Fe:Cu=3:6 must lead to some chemical disorder in the chains. Second, these cations take on local coordinations in the chain that are known to be slightly different. Unfortunately, powder x-ray diffraction lacks the sensitivity to establish details of structural order in the chains as also recognized by previous workers.[7,11] Fortunately, ^{57}Fe Mössbauer (Refs. 10, 16, and 17) and ^{63,65}Cu NMR/NQR (Ref. 18) spectroscopies can provide valuable information on chain-site occupancies thus complementing the x-ray structure results.

B. Site occupancies, oxygen content, and bulk superconductivity

The central result to emerge from the present work is the striking correlation between chain molecular structure, oxygen content and bulk superconductivity in the present YSCFO system. Specifically, the fraction of *C*-site occupancy in the chains $I_C/(I_C+I_A)$ deduced from Mössbauer spectroscopy measurements (Table I) is found to increase with the amount of bonded oxygen in the crystalline phase (Fig. 9) displaying two plateaus. For completeness we have included results on additional samples in Fig. 9. Details on sample preparation appear in Fig. 9 caption. At the first plateau, when the *C* site occupancy exceeds a critical value of $I_C/(I_C+I_A)=(I_c/I')_{cr}\simeq 0.47(1)$, bulk superconductivity manifests in the present cuprate system. The Meissner fractions are found to increase in proportion to $(I_C/I')-0.47$. These results suggest that presence of *A* sites (tetrahedral) in the chains, which proliferate in ambient pressure processed samples, suppress superconductivity in this trilayer structure.

Processing of the samples at high temperatures (900 °C) in a high oxygen pressure (27 MPa) ambient leads to an opening of the $Fe(O)_2(O_{1/2})_2$ tetrahedral units into trigonal bipyramidal ones by occupancy of an O(4) chain site in its vicinity and a concomitant displacement of the Fe(1) cation towards the center as schematically illustrated in Fig. 10(b). Once transformed, the *C* sites appear to be stable at ambient pressure. The role of high pressures and temperatures appears to be to facilitate the atomic scale transformation of $A\rightarrow C$ sites in bulk materials. Our results (Fig. 9) show that the variation of $I_C/(I_C+I_A)$ with oxygen content y in the range $6.5<y<7.1$ displays a pair of plateau's. The proposed model for $A\rightarrow C$ site transformation requires the uptake of one oxygen atom per iron atom to form a *C* site. Since 85% of the Fe dopant is localized in the chains, the predicted variation of site populations $N_C/(N_C+N_A)$ with y leads to a maximum slope of $1/(0.3\times 0.85)=3.92$ (broken line in Fig. 9) provided all added oxygen is Fe associated. We could not exclude the possibility that site f factors are unequal and that these increase with y. However, the close similarity in the slopes $d[I_C/(I_A+I_C)]/dy$ with that of the broken line is suggestive of a more attractive explanation.

In the oxygen concentration ranges of $6.75<y<6.9$ and $7.1<y<7.2$, the steep growth in $I_C/(I_C+I_A)$ displays a slope close to the maximum value of 3.9 (see Fig. 9). These results strongly suggest that in these oxygen concentration ranges, oxygen is principally absorbed at Fe-dopant *A* sites in the chains. On the other hand, in the oxygen concentration ranges where plateaus manifest, one is led to conclude that oxygen is absorbed at Cu(1) chain sites.

The subtle competition for chain oxygen between Fe and Cu cations revealed by the $I_C/(I_C+I_A)$ systematics of Fig. 9 can be qualitatively understood in terms of free-energy considerations of the doped system. Chemical bond energy considerations elucidated by Oesterreicher and Lee[19] suggest that at low oxygen content ($y<6.7$), Cu and Fe chain cations are present in Cu^1Cu^1 and Fe^2Fe^2 (pair of *A* sites) units. The underlying enthalpies of formation of such units are the highest of all possible fragments. The superscript on cations designate the number of oxygen nearest neighbors in the ab plane. With increasing oxygen content, Fe^2Fe^3 units (i.e., a pair of *A* and *C* sites) Cu^2Cu^1 units and Fe^3Fe^3 (i.e., a pair of *C* sites) are the preferred local units formed based on enthalpic considerations. We can thus trace the first plateau ($6.9<y<7.05$) to oxygen uptake at Cu sites in the chains to form Cu^2Cu^1 fragments, while the second plateau ($7.18<y<7.30$) to oxygen uptake to form the familiar Cu^2Cu^2 fragments (square-planar chain units) characteristic of the YBCO structure.

A particularly remarkable aspect of our results in Fig. 9, is the critical value of the ratio $I_C/(I_A+I_C)=0.47$ before bulk superconductivity onsets in the present YSCFO system. Trigonal bipyramidal coordinated Fe sites in the chains apparently promote superconductive coupling between the CuO_2 planes since the superconductive fractions in the samples steadily increase in proportion to $[I_C/(I_A+I_C)-0.47]$. We are also struck by the fact that the $T_c=60$ K of a 10% Fe-doped YSCO sample equals that of a pristine YSCO sample.[1] If $T_c=60$ K is truly representative of pristine YSCO, then in the doped samples, 30% replacement of the Cu cations in the chains by Fe has not only had no detrimental effect on T_c, but in fact, strongly promoted flux pinning as will be discussed later.

The plane-site occupancies (I_B/I) show a small but systematic reduction with oxygen content as revealed by the results of Table I. In absolute terms, there is $\sim$2.5 atomic percent of Fe dopant occupancy in the planes in the nonsuperconducting samples (*Q* and *A*) and about half that value (1.5 at. %) in the superconducting ones (*O* and HPO3). The presence of Fe dopant in the planes most likely serves to suppress the superconducting state by depairing the carriers. At the same time, since I_B/I remains unchanged between samples *O* and HPO3, the significant increase in diamagnetism (Fig. 4) between these samples could not be directly related to Fe (*B* site) occupancy in the planes in the present case.

We have also examined[20] grain-aligned YSCFO samples at 300 and at 4.2 K to ascertain the local magnetic field, sign and direction of V_{zz} for sites *A*, *B*, and *C*. The experiments reveal a negative V_{zz} tilted somewhat with respect to the *c* axis for both sites *A* and *C*. These results will be dealt with in a forthcoming publication.[20]

C. Role of local structure and superconductivity in YSCO and YBCO

An issue of central importance within context of pairing of carriers in the present layered cuprates is the role of local structure. Zn- and Ga-doping experiments in YBCO (Ref. 21) in this regard, have been particularly insightful since both dopants enter the trilayered structure, tetrahedrally co-

ordinated to four oxygen near neighbors thus leaving the oxygen content of the doped material unchanged at 7. Zn dopant is thought[22] to localize in the planes, while Ga dopant localizes in the chains. The steeper decrease of T_c with doping concentration x for Zn ($dT_c/dx = 6.4$ K/at. %) than for Ga ($dT_c/dx = 2.5$ K/at. %) is generally ascribed[21] to the more important role of the CuO_2 planes than CuO_3 chains to support superconducting carriers in these cuprates.

The Ga-doping experiments in YBCO (Ref. 21) and YSCO (Ref. 3) are insightful for another reason, these provide a baseline to establish the detrimental effect of replacing square planar $CuO_2(O_{1/2})_2$ units by tetrahedral $GaO_2(O_{1/2})_2$ ones at a fixed oxygen stoichiometry. For example, in $YBa_2(Cu_{1-x}Ga_2)_3O_7$ and $YSr_2(Cu_{1-x}Ga_x)_3O_7$, with x increasing to 0.10, T_c drops from 91 to 65 K in the former and from 60 to 21 K in the latter cuprate.

It is instructive to draw an analogy between the role played by Fe (A site) dopant and Ga dopant in suppressing superconductivity of YSCO. Both these cations are tetrahedrally coordinated in the chains and suppress T_c in an approximate proportion to their occupancies in the chains. Thus replacement[3] of 30% Cu(1) sites by Ga in the chains reduced T_c of YSCO from 60 to 21 K, while the replacement of about one half of the 30% Cu(1) sites by Fe A sites in the chains reduces T_c of YSCO to 28 K. It is also worth rescaling that high-pressure oxygen annealing of a $YSr_2Cu_{2.7}Ga_{0.3}O_y$ sample leaves the $T_c = 21$ K unchanged,[3] most likely because the Ga^{3+} dopant is resistant to further oxidation and continues to be tetrahedrally coordinated in the chains. On the other hand, high-pressure oxygen annealing of a $YSr_2Cu_{2.7}Fe_{0.3}O_y$ sample leads to a qualitative enhancement of superconductivity which is accompanied by a nearly complete change in local structure of Fe dopant in the chains (from tetrahedral to nontetrahedral coordination) as strikingly demonstrated by the present Mössbauer studies. These studies highlight, in an elegant fashion, the crucial role of local structure rather than the average structure in controlling the superconductive behavior of the layered cuprates.

It is reasonable to think that trilayer fragments composed of a pair of CuO_2 planes separated by either square-planar Cu(1) sites or distorted trigonal bipyramid Fe C sites but not tetrahedral Fe A sites are spontaneously superconducting. It is then of interest to inquire if the observed threshold for onset of bulk superconductivity (Fig. 9) in YSCFO represents a percolation threshold. In the range $6.9 < y < 7.05$, where the first plateau occurs, if we take one-half of all Cu(1) sites to be square planar as suggested by the Cu^2Cu^1 configuration (Ref. 19) discussed in Sec. III B, then the observed value of $I_C/(I_A+I_C) = 0.47$ (Fig. 9) translates into a nontetrahedral (superconducting) chain-site fraction of ~ 0.47. This threshold is surprisingly close to the threshold of 0.50 for bond percolation and somewhat lower than the threshold of 0.59 for site percolation in a two-dimensional (2D) network.[23] These ideas can be refined in the future as details of Cu(1) local order in such samples can be reliably ascertained from ^{65,63}Cu NQR/NMR (Ref. 18) and extended x-ray absorption fine-structure studies.

D. Flux pinning and origin of secondary peak in magnetization hysteresis of Fe-doped YSCO samples

The recent observation[24–27] of a secondary peak (fishtail) in magnetization $M(H)$ hysteresis loops in several single crystals of high-T_c based cuprates and melt-grown Nd- and Sm-based 123 materials has stimulated interest in understanding the origin of such a peak. Several workers[24–26] have favored intrinsic heterogeneity of oxygen content in such samples as a source of flux pinning contributing to the secondary peak. An alternate view[27–29] is that the fishtail magnetization represents evidence of a dimensional crossover at a temperature T_{cr}, with quasi-2D vortex fluctuations prevailing at $T < T_{cr}$, and 3D vortex fluctuations prevailing at $T > T_{cr}$. At the crossover temperature T_{cr}, the fishtail magnetization disappears[27] and concomitantly the irreversibility field H_{irr} displays a change in functional form from an exponential dependence as a function of T (at $T < T_{cr}$) to a power-law behavior $\alpha(1-T/T_c)^n$ with n in the range $3/2 \leqslant n \leqslant 2$ (at $T > T_{cr}$). These functional forms have been derived assuming Lindemann's melting criterion[26,27] as applied to the flux lines in 2D and 3D.

The magnetization hysteresis loops in the present YSCFO samples (HPO3) shown in Fig. 5, display a secondary peak in the irreversible magnetization which is discernible at $T < 55$ K. The high flux-pinning in HPO3 samples where C sites proliferate has been noted before[30] for the corresponding Ba analog in samples synthesized at ambient pressure. A plot of $\log_{10}\Delta M$ (irreversible magnetization at the secondary peak) against T [Fig. 6(a)] reveals a linear behavior at low T ($T \lesssim 45$ K) and a sharper change at high T (45 K $< T <$ 60 K). The low-T results imply that ΔM decreases exponentially with T. At higher temperatures, a plot of $\log_{10}H_{irr}$ against $\log_{10}(1-T/T_c)$ reveals a power-law behavior with $n = 2.16(5)$ as illustrated in Fig. 6(b). Our results on the HPO3 sample thus reveal a change in the functional form describing ΔM with T near $T = 45$ K, which we identify with the crossover temperature T_{cr}. These features of our magnetization results are suggestive that the fishtail magnetization is an intrinsic behavior of the system resulting due to a dimensional crossover of flux pinning from 2D to 3D with increasing T. It is difficult to imagine that these magnetization results arise due to extrinsic effects such as heterogeneity of oxygen content. It would be well to recall here that the present polycrystalline HPO3 samples, possess a small grain size (5 μ) and were treated in oxygen both at ambient pressure and at high pressures for extended periods ($>$24 h).

IV. CONCLUSIONS

Magnetization and ^{57}Fe Mössbauer spectroscopy measurements on $YSr_2Cu_{2.7}Fe_{0.3}O_y$ samples studied as a function of oxygen content have shown a close connection between onset of bulk superconductivity and chain-molecular structure. In particular, when the C-site (trigonal bipyramidally coordinated Fe in the chains) occupancy $I_C/(I_A+I_C)$ exceeds a critical value of 0.47(1), bulk superconductivity manifests. A model is developed for the A-site (tetrahedrally coordinated Fe in the chains) to C-site transformation upon oxygen uptake which is not only in harmony with the microscopic site (A,C) assignments, but quantitatively describes the observed variation of chain-site occupancies $[I_C/(I_C+I_A)]$ as a function of sample oxygen content. In samples synthesized by annealing at 915 °C and at 27 MPa oxygen pressure, a nearly complete transformation of $A \rightarrow C$ sites is observed, i.e., $I_C(I_A+I_C) = 0.91$. In such samples, processed at high oxygen pressures, not only is

$T_c = 60$ K, characteristic of the pristine $YSr_2Cu_3O_7$ material, but a shielding fraction close to 100% is obtained at low fields. At higher fields a secondary peak in the irreversible magnetization is observed indicative of flux pinning in a quasi-2D lattice at $T < 45$ K with evidence of a dimensional crossover to 3D at $T > 45$ K.

ACKNOWLEDGMENTS

It is a pleasure to acknowledge discussions with Professor Richard Zallen and Professor Bernard Goodman during the course of this work. This work was supported by National Science Foundation Grant No. DMR-93-09061.

[1] Bin Okai, Jpn. J. Appl. Phys. **29**, L2180 (1990).
[2] P. R. Slater and C. Greaves, Physica C **180**, 299 (1991).
[3] T. Den and T. Kobayashi, Physica C **196**, 141 (1992).
[4] S. A. Sunshine, L. F. Schneemeyer, T. Siegrist, D. C. Douglass, J. V. Waszczak, R. J. Cava, E. M. Gyorgy, and D. W. Murphy, Chem. Mater. **1**, 331 (1989).
[5] M. G. Smith, R. D. Taylor, and J. D. Thompson, Physica C **208**, 91 (1993).
[6] Q. Xiong, Y. Y. Xue, J. W. Chu, Y. Y. Sun, Y. Q. Wang, P. H. Hor, and C. W. Chu, Phys. Rev. B **47**, 11 337 (1993).
[7] M. Pissas, G. Kallias, E. Moraitakis, D. Niarchos, and A. Simopoulous, Physica C **234**, 127 (1994). V. Terziev, R. Suryanarayanan, Mamidanna, S. R. Rao, L. Ouhammou, O. Gorochov, and J. L. Dorman, Phys. Rev. B **48**, 13 037 (1993).
[8] J. M. Tarascon and B. G. Bagley, in *Chemistry of Superconductor Materials*, edited by T. Vanderah (Noyes, Park Ridge, NJ, 1992), p. 310.
[9] Y. Wu, S. Pradhan, and P. Boolchand, Phys. Rev. Lett. **67**, 3184 (1991). Y. Wu, Ph.D. thesis, University of Cincinnati, 1994.
[10] P. Boolchand and D. McDaniel, in *Studies on High Temperature Superconductors*, edited by A. V. Narlikar (Nova Science, New York, 1990), Vol. 4, 143; Hyperfine Interact. **72**, 125 (1992).
[11] A. Rykov, V. Caignaart, and B. Raveau, J. Solid State Chem. **109**, 295 (1994).
[12] L. Bottyan, J. Dengler, Gy. Faigel, N. E. Kaner, D. L. Nagy, G. Ritter, and U. Röhlich, Hyperfine Interact. **93**, 1647 (1994).
[13] J. Dengler, G. Ritter, G. Saemann-Ischenko, B. Roas, L. Schultz, B. Molnar, D. L. Nagy, and I. S. Szücs, Hyperfine Interact. **55**, 1267 (1990).
[14] P. Boolchand, S. Pradhan, Y. Wu, M. Abdelgadir, W. Huff, D. Farrell, R. Coussement, and D. McDaniel, Phys. Rev. B **45**, 921 (1992).
[15] J. D. Jorgensen, M. A. Beno, D. G. Hinks, L. Soderholm, K. J. Volin, R. L. Hitterman, J. D. Grace, I. K. Schuller, C. U. Segre, K. Zhang, and M. S. Kleefish, Phys. Rev. B **36**, 3608 (1987); Also see R. J. Cava, A. W. Hewet, B. Batlogg, M. Marezio, K. M. Rabe, J. J. Krajewski, W. F. Peck, Jr., and L. W. Rupp, Jr., Physica C **165**, 419 (1990).
[16] V. Chechersky and A. Nath, Hyperfine Interact. **72**, 173 (1992); I. S. Lyubutin, S. T. Lin, C. M. Lin, T. V. Dmitrieva, K. V. Frolov, A. M. Balagurov, F. Bouree, and I. Mirebeau, Physica C **248**, 222 (1995); **248**, 235 (1995).
[17] I. Felner and I. Nowik, Supercond. Sci. Tech. **8**, 121 (1995); M. E. Lines and M. Eibschutz, Physica C **166**, 235 (1990).
[18] D. Brinkmann, Z. Naturforsh. **44a**, 393 (1990); C. H. Pennington, D. J. Durand, D. B. Zaxc, C. P. Slichter, J. P. Rice, and D. M. Ginzburg, Phys. Rev. B **37**, 7944 (1988).
[19] H. Oesterreicher and Ju-Yeol Lee, Mater. Res. Bull. **27**, 1125 (1992).
[20] P. Boolchand, F. Shi, W. J. Bresser, R. Enzweiler, B. Goodman, D. McDaniel, and D. Farrell, Bull. Am. Phys. Soc. **41**, 98 (1996).
[21] G. Xiao, M. Z. Cieplak, D. Musser, A. Gavrin, F. H. Streitz, C. L. Chien, J. J. Rhyne, and J. A. Gotaas, Nature (London) **332**, 238 (1988).
[22] J. C. Phillips, Solid State Commun. **81**, 497 (1992); also, see, J. C. Phillips, *Physics of High-T_c Superconductors* (Academic, New York, 1989), p. 98.
[23] R. Zallen, *The Physics of Amorphous Solids* (Wiley, New York, 1983), p. 168.
[24] M. Murakami, S. I. Yoo, T. Higachi, N. Sakai, J. Weltz, N. Koshizuka, and S. Tanaka, Jpn. J. Appl. Phys. **33**, L715 (1994).
[25] S. I. Yoo, N. Sakai, H. Takaichi, T. Higuchi, and M. Murakami, Appl. Phys. Lett. **65**, 633 (1994).
[26] M. Darumling, J. M. Seuntjens, and D. C. Larbalestier, Nature (London) **346**, 332 (1990).
[27] F. Zuo, S. Khizroev, G. C. Alexandrakis, and V. N. Kopylov, Phys. Rev. B **52**, R755 (1995); also see A. Schiling, R. Jin, J. D. Guo, and H. R. Oh, Phys. Rev. Lett. **71**, 1899 (1993).
[28] F. Lindemann, Z. Phys. **11**, 69 (1910).
[29] D. E. Farrell, J. P. Rice, and D. M. Ginzburg, Phys. Rev. Lett. **67**, 1165 (1991).
[30] M. G. Smith, H. Oesterreicher, M. P. Maley, and R. D. Taylor, Physica C **204**, 130 (1994).